ISSN 0016-8521, Geotectonics, 2010, Vol. 44, No. 2, pp. 139–157. © Pleiades Publishing, Inc., 2010.
Original Russian Text © S.Yu. Kolodyazhny, 2010, published in Geotektonika, 2010, Vol. 44, No. 2, pp. 56–76.

Structural and Kinematic Assemblies in Sedimentary Rocks of the Phanerozoic Cover of the Mid-Russian Dislocation Zone

S. Yu. Kolodyazhny

Geological Institute (GIN), Russian Academy of Sciences, 7 Pyzhevskii per., Moscow, 119017, Russia
e-mail: kolod@ginras.ru

Received January 1, 2009

Abstract—The Mid-Russian Dislocation Zone is a large within-plate structural element of the East European Platform, which extends for more than 1100 km from the Timan Foredeep to the Orsha Basin. This deep, long-lived zone was formed against a background of changeable geodynamic settings, including (1) Late Paleoproterozoic collision events, (2) Late Riphean–Early Vendian epicontinental rifting, (3) Late Vendian–Early Triassic intraplatform tectogenesis with formation of horst-like uplifts within the zone against the background of general subsidence, and (4) Mesozoic–Cenozoic within-plate reactivation. At the final Kimmerian–Alpine stage of its evolution, the Mid-Russian Zone developed as a left-lateral transpressional structure with penetrative dissipative shear deformation resulting in the general horizontal transfer of Phanerozoic sedimentary rocks. The dislocations were manifested as two dynamically conjugate structural forms: a zone of scattered shearing and a bedding-plane tectonic flow. The dynamic manifestation of the Mid-Russian and the conjugate Belomorian–Dvina zones, which make up a common arcuate structure (in plan view), allowed us to outline the Dvina–Sukhona plate-flow with horizontal mass transfer in the southeastern direction. The tectonics of the Mid-Russian Dislocation Zone is considered in this paper with particular emphasis on the structural and kinematic assemblies in sedimentary rocks of the Phanerozoic cover.

DOI: 10.1134/S0016852110020044

INTRODUCTION

In plate-tectonic reconstructions, lithospheric plates are considered to be monolithic structural elements that undergo considerable lateral movements without substantial modification of their infrastructure. The active boundaries of plates (collision belts, spreading zones, etc.) are regarded as the main sources and attractors of tectonic processes, and these boundaries have attracted widespread attention. Geological practice, however, shows that large hydrocarbon fields and base-metal, diamond, and other mineral deposits are localized in within-plate regions. Perhaps because of this, a gap exists between theoretical and applied tectonics, which are based on different principles and show different interests.

Recent data indicate the internal volumetric mobility of lithospheric plates, including those underlain by ancient continental crust. Various methods have been used to establish that lateral displacements within different layers of tectonically delaminated crust and upper mantle are prevalent forms of within-plate tectogenesis [9, 11–13, 15–18, 25]. These data do not conflict with the global plate-tectonic concept but only supplement it, imparting the character of 3D tectonic flow to this model. A new paradigm of volumetric mobility inherent to lithospheric plates is combined with practical developments concerning the formation of hydrocarbon fields in 3D-deformed crystalline complexes [15]. Thus, the study of within-plate structural elements related to horizontal displacements is of great theoretical and practical importance.

The East European Platform (EEP), or subplate, is one of the most important objects of within-plate tectonics. Data on stress fields and seismicity, as well as general structural and tectonic investigations, have revealed substantial deformations of this plate related to its horizontal movements and interaction with the adjacent mobile belts and plates [12, 14, 17, 18, 25]. Many unsolved problems remain with respect to the character of the displacement of the EEP as a monolithic plate or a mosaic of subplate blocks, the within-plate structural assemblies pertaining to horizontal offsets, and the debatable mechanisms of stress transmission for many hundreds of kilometers from the active plate boundaries.

New structural and kinematic data shed light on some of the above issues. Study of the northeastern EEP, including the southeastern Baltic Shield and the vast adjacent portion of platform cover revealed a complex, long-lived structural assembly that evolved in the basement–cover system [9, 11]. It was noted that Paleoproterozoic tectonic disturbances in the Precambrian basement underwent multifold subsequent remobilization and penetrated into the sedimentary cover in the form of a reflected structural assembly having specific characteristics. This phenomenon is manifested in structural elements of various ranks, including extended mobile belts and rifts,

separate faults and fracture zones, up to the mesostructural elements observed at outcrops.

The tectonics of the Phanerozoic cover in the northeastern segment of the Mid-Russian Dislocation Zone, one of the main structural elements of the EEP, is considered in this paper. The deformations revealed in the Paleozoic and Mesozoic sedimentary rocks at a great distance from the active plate boundaries are a phenomenon that merits detailed study.

KINEMATIC ANALYSIS OF PLATFORM STRUCTURAL ELEMENTS: METHODICAL ASPECTS

The general technique of structural and kinematic analysis was considered in [10]. The specificity of the structural study of platform cover is determined by the physical properties of the rocks, the thermodynamic regime of deformation, and their low intensity. In many cases, researchers deal with poorly manifested structural elements at the incipient stage of their development. On the one hand, the near-surface character of deformation facilitates brittle failure of rocks, and on the other hand, nonuniform epigenetic alteration of sediments results in the formation of bedded and more complex, rheologically contrasting media formed by rocks of variable viscosity.

A combination of plastic clay, poorly cemented sand, and highly competent rocks (dolomite, sandstone, etc.) gives rise to the situation where the structures of ductile and granulated flow, brittle failure, and block sliding develop contemporaneously in the common stress field. This situation facilitates redistribution of deformations: stresses relax mainly in the plastic layer, while in the adjacent viscous layers deformation is either lacking or manifested in structural elements distinct in type and orientation. The refraction at the boundaries of the layers differing in competence results in variation of the spatial position of the planar structural elements. For example, in many cases, the dip angles of the faults change sharply. In plastic beds, these are thrust–strike-slip faults, whereas penetrating into competent beds, they are transformed into strike-slip and reverse faults. A complex combination of wrench faults in viscous beds with zones of bedding-plane detachments and flow in the adjacent plastic interbeds is typical. These features lead to the appearance of disharmony and false structural unconformities between the units of different rheological properties, as well as to the false impression of multiphase deformation based on diversity of ductile deformation and brittle failure, which actually make up a single dynamic assembly. Kinematic analysis requires that these factors be taken into account.

In the course of investigation, remote sensing was used, including the interpretation of digital topographic maps (satellite altimetry), aerial photographs, and satellite images. Of the multitude of revealed lineaments, those fracture systems have been chosen which are linked to the cover and basement structural elements depicted in the contour lines and configuration of gravity and magnetic anomalies. The preliminary kinematic identification of faults was based on the interpretation of the structural patterns in plan view [1, 12, 19. 20]. The results of remote sensing were verified by ground observations.

The results of fieldwork were summarized in the form of integral diagrams demonstrating the spatial combinations of structural elements. The kinematically coherent assemblies were selected from them. The fracture systems that make up the shear deformation zones are very informative[1]. Their regular combinations typically comprise master faults (L or C) and auxiliary splays: synthetic (Riedel shears R and P) and antithetic (R' and X), tension cracks (T) and compression structural elements (F, S) (Fig. 1a). The master faults are identified from deformation gradients in the linear fracture zones, where the density of fractures, as a rule, parallel to master faults, increases toward the latter.

The spatial position of the auxiliary structural elements in various segments of the master strike-slip fault is variable. In the segments of waning, a horsetail pattern with regular arrangement of tension and compression structures or a system of radial and concentric fractures is formed (Fig. 1b, mega- and macrolevels). Segments of bending and echeloned buildup of strike-slip faults are accompanied by connecting bridge structures of extension and compression, in particular, by pull-apart mini-structures.

The combinations of structural elements at the meso- and microlevels are distinguished by asymmetry that allows determination of the kinematics of disturbance. The intense deformation in the strike-slip zone results in the formation of mylonites with asymmetric C–S microstructures characterized by a combination of S-shaped schistosity and sliding C-planes (Fig. 1b, meso- and microlevels).

At the mesolevel of observations, it is difficult to determine the kinematic type of auxiliary shear in the absence of explicit offsets and any other components of assembly. In this case, it is helpful that near-surface dislocations in cover develop nonuniformly and make it possible to detect the segments of their embryonal development and progressive transition to zones of intense dislocations. According to experimental data [31], the shear fractures develop in the following sequence: (1) synthetic Riedel shears R and conjugating compression bridge structures; (2) synthetic Riedel shears P and accompanying extension "bridges"; (3) incipient boudinage as a result of intersection of R and P shears; (4) master L shears, whose

[1] The term *shear deformation zone* has a mechanical sense and is used in contrast to the term *strike-slip dislocation zone* in the geological sense (in short, strike-slip zone), which is applied to steeply dipping zones of faulting and folding related to strike-slip offsets [10].

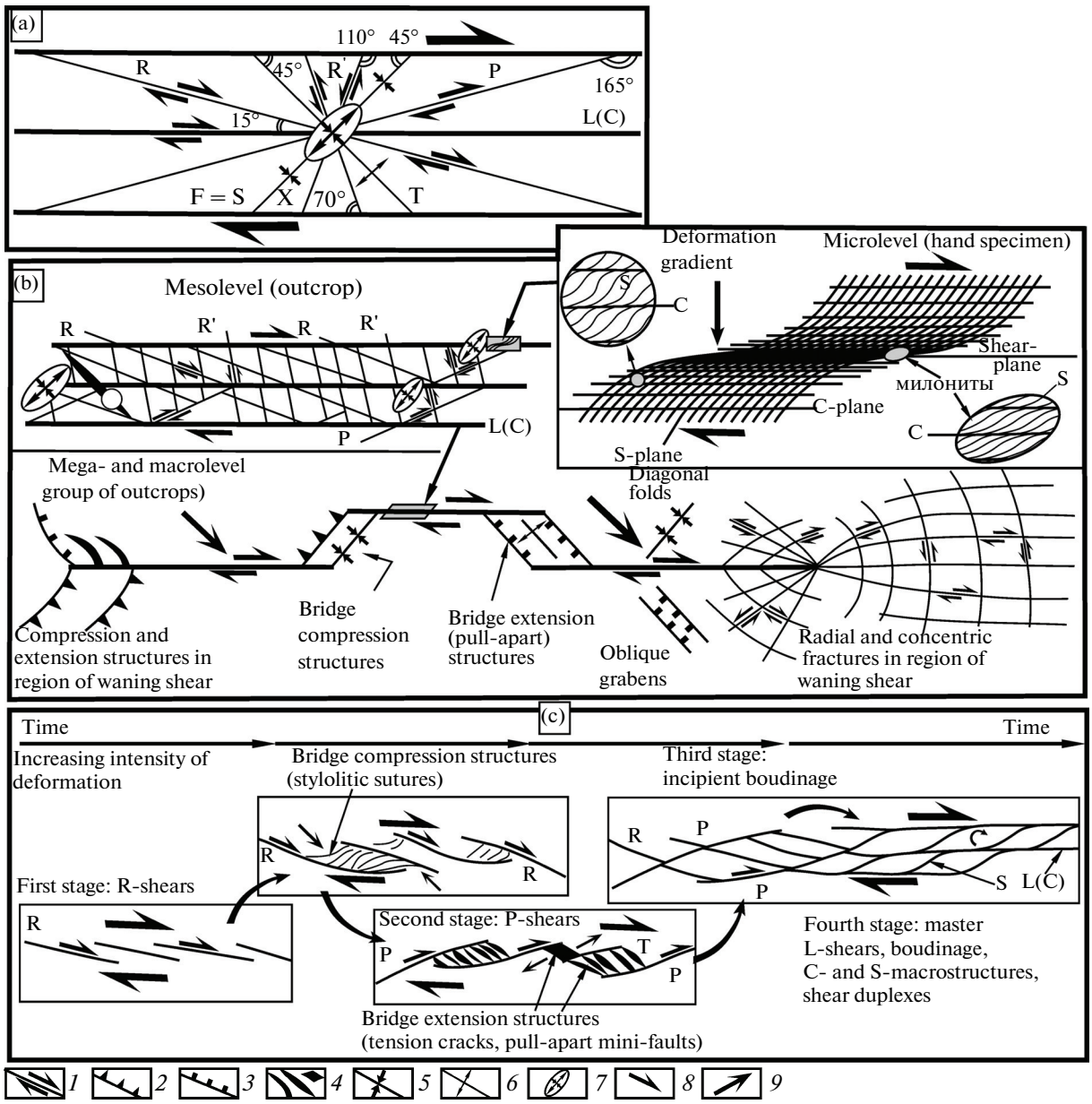

Fig. 1. Principles of kinematic interpretation of structural assemblies in zones of shear deformation: (a) classification of Riedel shears [10, 13], (b) spatial relationships of conjugate structural elements for various segments and scale levels of strike-slip fault zones, and (c) progressive development of structural evolution in strike-slip fault zones in the course of deformation; data from [31] are used. (*1*) Strike-slip fault; (*2*) reverse and thrust faults; (*3*) normal fault; (*4*) tension crack; (*5, 6*) structural elements of (*5*) compression and (*6*) extension; (*7*) orientation of principal axes of deformation ellipsoid; (*8, 9*) direction of (*8*) strike-slip and (*9*) tangential offsets. Letters in the figure: L, C, master strike-slip faults; R, P, auxiliary synthetic shears; R', X, auxiliary antithetic shears; T, extension structural elements (tension cracks); F, S, compression structural elements: F, folds and S, schistosity.

progressive development controls asymmetric boudinage, C–S meso- and microstructures, as well as the phenomena related to the rotation of linear and planar structural elements relative to the shear plane (Fig. 1c). Eventually, a completely developed zone of shear deformation with regular asymmetric structure allows estimation of the displacement type. Thus, the structural relationships between auxiliary shears reflect the sequence of their formation.

Field observations support the experimental data. The shear deformation zones commonly develop as dashed segments with progressive buildup of each segment along the strike up to their merging into a continuous fracture. Where particular segments are waning, the series of auxiliary shears can be revealed and identified in their primary succession. Systems of auxiliary fractures at the initial stage of shearing are also noted off the axial part of shear deformation zones in

the region of their dynamic effect and gradual waning. In other words, the stages in development of shears are expressed not only in their chronological relationships but also in their deformation intensity. Thus, the kinematic identification of auxiliary fractures is deduced from their spatial arrangement and the asymmetry of their localization.

The morphology of slickenside surfaces is an important kinematic guide as well [12, 24, 30]. These structural elements are, however, poorly preserved, owing to kinematic inversions along the fracture planes. Commonly, several gently dipping striation systems testify to strike-slip displacements, but the morphology of the steps and other morphological indicators are often distorted due to the superposition of subsequent shearing. Thus, this technique, sensitive to tectonic displacements, was used only to supplement the criteria based on asymmetry of the shear zones (see above), which mark the most significant kinematic events. The kinematics of particular fractures and high-order shear zones was studied using a complex approach that included documentation of offsets along the reference structural elements and bending of planar structures along the fault planes, the morphology of C–S structures and slickensides, and the asymmetry of dislocation zones. The statistical processing was performed using structural diagrams that reflect the main kinematic features of particular dislocation zone segments.

The results of remote sensing and field observations were displayed in structural and kinematic schemes that served as the basis for dynamic interpretation.

The structural investigations of sedimentary cover in the northern EEP affected by Quaternary glaciation require distinguishing between tectonic and glacial dislocations. This issue was considered in [13] and is discussed below, where specific structural elements are described.

GENERAL TECTONIC FEATURES OF THE MID-RUSSIAN ZONE

The Mid-Russian Dislocation Zone is a large transplatform structural element that extends for more than 1100 km from the Timan Foredeep in the northeast to the Sukhona River basin and the Rybinsk water reservoir, and further to the headwater of the Volga River and the Orsha Basin in the southwest (Fig. 2a). The width of this zone and its outlines vary with depth. In the crystalline basement, a wide (200–500 km) belt, clearly expressed in gravity and magnetic fields and considered a collision tectonic unit formed in the Late Paleoproterozoic [5, 8, 21, 22], corresponds to this zone. The continental crust is thinned here (34–38 km, compared to 38–44 km in the adjacent blocks) due to the postcollision reduction of the upper granitic–gneissic layer and is characterized by high-velocity ($V_p > 7.2$ km/s) material of the crust–mantle mixture at the bottom of the lower crust [5].

At the crystalline basement surface, the contours of the zone are controlled by a system of grabens filled with Upper Riphean and Lower Vendian continental terrigenous rocks and making up the complexly built Mid-Russian Aulacogen [3, 28] (Fig. 2a). Separate Riphean grabens are en-echelon arranged, displaced along the transverse faults, and typically comprise two main troughs separated by a basement salient. The widths of these troughs decrease from the southwest to the northeast. They converge in this direction and eventually merge into a single graben-like structural unit near the city of Kotlas. The depth of tectonic downcutting of the troughs increases in the same direction. If in the southwestern segment of the aulacogen the basement depth at the graben bottom is 1200–1500 m, then near Kotlas it reaches 5000–6000 m [28]. As follows from the drilling results and the seismic data indicating the decrease in V_p of the crystalline complexes [5, 28], the basement rocks beneath the Riphean grabens underwent destruction and cataclasis. The northeastern segment of the Mid-Russian Aulacogen differs from the southwestern segment in thickness and structure of the Riphean stratigraphic section and intensity of dislocations. In the segment from Vologda to Kotlas, the narrowing of the aulacogen in plan view is accompanied by concentration of deformation and increase in the amplitude of displacement (up to 2000 m) along the boundary normal faults.

The Upper Vendian sedimentary rocks overlap the deeply eroded Riphean structures of the Mid–Russian Aulacogen and seal it. The Late Vendian transgression opens the platform stage of evolution of the EEP, when sedimentary cover was deposited with the formation of the Moscow Syneclise that partly inherited the spatial position of the Paleoproterozoic Mid-Russian Belt. The tectonic style of the sedimentary cover appreciably differs from the tectonics of the lower structural stages, though in general, many structural elements of the plate megacomplex inherited tectonic elements of the basement. In particular, the inheritance is expressed in swell-like inversion structures directly above the rifts of the Mid-Russian Aulacogen.

This situation is especially striking in the northeastern segment of the Mid-Russian Dislocation Zone, whose axial part is marked by the Rybinsk–Sukhona Megaswell that crowns the northern branch of the Mid-Russian Aulacogen (Fig. 2b). This structural element is composed of all cover units, but the amplitude of the uplift decreases upsection from 1000–300 m at the bottom of the cover to 300–50 m at the stratigraphic levels, beginning from the Ordovician roof [2]. The megaswell is complicated by auxiliary folds and swells, which are traps for hydrocarbons, in combination with faults. According to geophysical data, the latter are interpreted as reverse faults with a separation reaching 1000 m at the lower stratigraphic units and gradually decreasing to a few hundreds and tens of meters upsection [2, 5]. Many such faults inherit

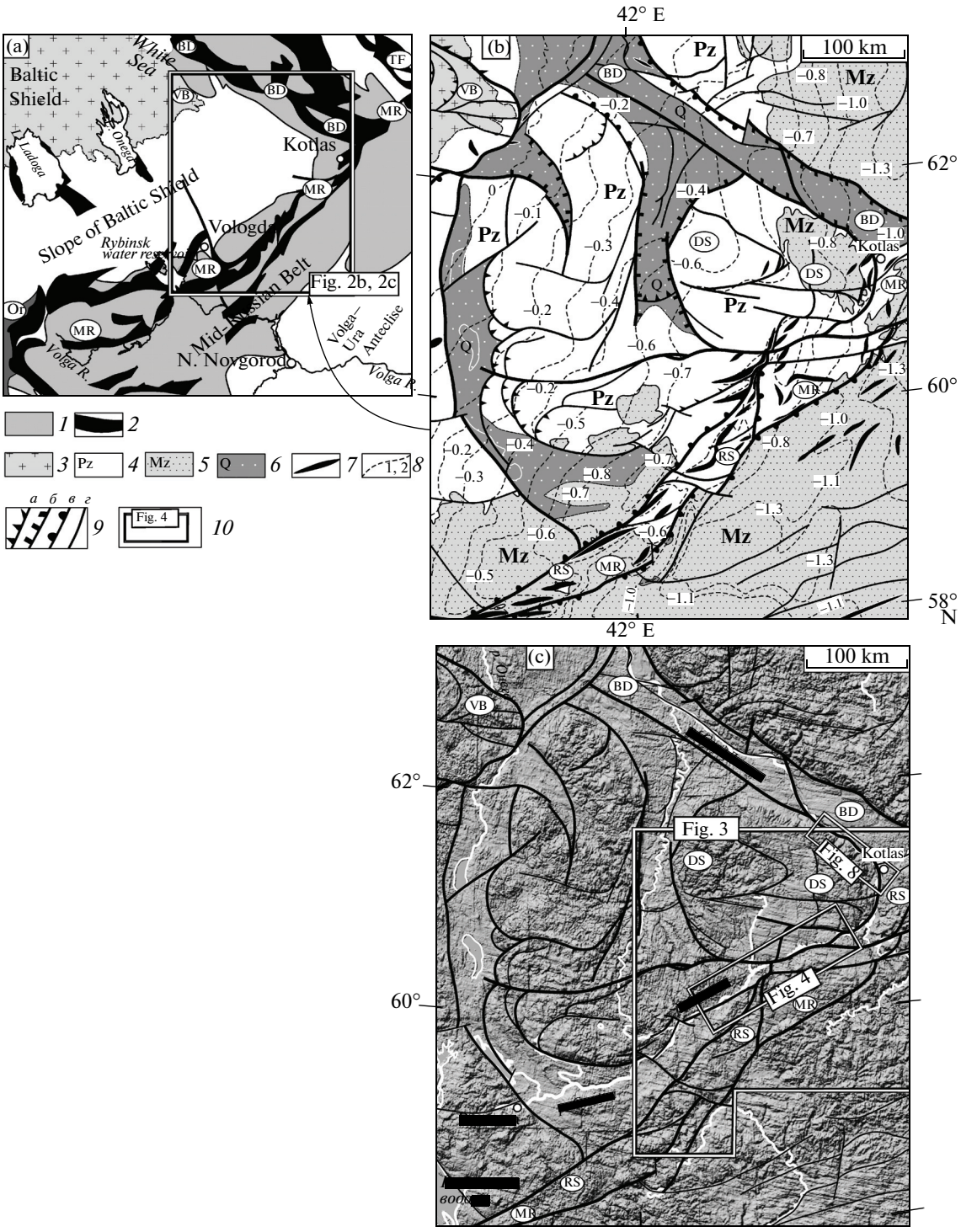

Fig. 2. (a) Position of the Paleoproterozoic Mid-Russian Belt and the Riphean system of aulacogens, compiled using the data from [3, 5, 7, 8]; (b) tectonic scheme of the Phanerozoic cover in the northeastern EEP, compiled using the data from [5, 7, 26]; (c) interpretation of digital topographic maps and satellite images of the northeastern EEP.

Panel (a): (*1*) Paleoproterozoic collisional belt, (*2*) Riphean aulacogen; panel (b): (*3*) Precambrian basement; (*4, 5*) sedimentary cover: (*4*) Paleozoic and (*5*) Mesozoic; (*6*) recent tectonic depression; (*7*) swell or anticline; (*8*) contour lines of the roof of the Vereya Unit of the Moscovian Stage, Middle Carboniferous; (*9*) fault zones: (*a*) reverse and thrust, (*b*) normal, (*c*) steeply dipping fault or flexure (half-spheres are directed toward subsided wall), (d) other, including wrench faults; (*10*) sites of detailed study shown in other figures. Abbreviations in figure. Dislocation zones: MR, Mid-Russian; BD, Belomorian–Dvina; blocks: DS, Dvina–Sukhona, VB, Vetreny Belt; RS, Rybinsk–Sukhona Megaswell, Or, Orsha Basin, TF, Timan Foredeep.

faults, which bound the Riphean grabens of the Mid-Russian Aulacogen in the basement, and thus are a result of rift structure inversion and transformation of ancient normal faults into reverse faults of the plate stage [2].

According to [2, 5], four rock complexes make up the sedimentary cover of the Moscow Syneclise: Upper Vendian–Lower Cambrian (Upper Baikalian), Middle Cambrian–Lower Silurian (Caledonian), Devonian–Lower Triassic (Hercynian), reduced Middle Jurassic–Cretaceous (Kimmerian), and Neogene–Quaternary (Alpine). The total thickness of the plate complexes in the Mid-Russian Zone reaches 2.0–3.5 km. They are all separated by regional unconformities and breaks in sedimentation comparable with epochs of tectonic rearrangements. Each complex reveals indications of synsedimentation growth of local uplifts and basins marked by variations in the thickness of sediments and the appearance of local surfaces of scouring and stratigraphic hiatuses.

The lithostratigraphic features show that the Rybinsk–Sukhona Megaswell periodically emerged against the background of sedimentation [2, 5, 23]. The largest amplitude of emergence (from 100 to 600–1000 m) was reached during the Kotlas–Baltic phase (Late Vendian–Early Cambrian) [2, 23], when the megaswell was a system of horst-like uplifts in the subsiding axial part of the Late Baikalian Moscow Syneclise. During the Caledonian epoch, the uplifting was decelerated and was partly compensated by deposition of Middle Cambrian–Lower Silurian sedimentary rocks. No intense uplifting is noted for the Hercynian epoch. The Middle and Upper Paleozoic sections of the megaswell reveal local surfaces of scouring and breaks in sedimentation combined with indications of local subsidence. The troughs were filled with Artinskian–Kungurian evaporites, upper Tatarian lacustrine and alluvial red beds, and Induan molassoids. The active regeneration of the Rybinsk–Sukhona Megaswell occurred in the Kimmerian–Alpine epoch, when the amplitude of uplifting reached 100–200 m [2, 5]. In the uplifted areas, sediments of this age are typically absent. Only Quaternary glacial and postglacial sediments are retained in the axial part of the megaswell, and Middle Jurassic–Lower Cretaceous rocks are locally known along its southeastern wall. Signs of Mesozoic magmatic events probably related to the inferred kimberlite province [27] are noted in the Mid-Russian Zone.

The neotectonic reactivation of the Rybinsk–Sukhona Megaswell is emphasized by the structure of the Sukhona River valley. To the west of the uplift, at the headwater of this river, the aggradational valley has gentle walls. During spring tides, the stream often changes its direction here and flows away from the megaswell. In the middle and lower reaches, where the Sukhona River crosses the Rybinsk–Sukhona Megaswell, its valley becomes erosional and actively cuts down sedimentary rocks, locally transforming into a canyon with steep cliffs up to 80 m high [4]. The neotectonic activity of the megaswell is accentuated by a system of lineaments expressed in present-day topography and traced in digital topographic maps (Fig. 2c). Judging from the contour lines of various stratigraphic units, most lineaments penetrate into the Riphean grabens and the basement rocks (Figs. 2a, 2b). Their neotectonic mobility and high permeability are supported by highly mineralized springs confined to the fault zones that drain salt-bearing units and by anomalous helium field. The He concentration in the subsurface water along the main faults of the Mid-Russian Dislocation Zone exceeds 20×10^{-5} mg/l [5].

All these data show that the Mid-Russian Zone is a long-lived structural element expressed in the present-day topography, the structure of sedimentary cover, the topography of the basement roof, and the structure of the Precambrian complexes deep in the crust (Figs. 2a–2c).

The tectonic activity of this structural element has periodically changed against the background of variable tectonic settings in the Late Paleoproterozoic, Riphean, Vendian–Paleozoic, and Mesozoic–Cenozoic [2, 4, 5, 7, 21, 22, 28]. The study of the evolution of this structural unit is of both scientific and practical importance because hydrocarbon fields and diamond-bearing complexes may be localized therein. This paper is aimed at comprehensive kinematic consideration of the postsedimentation structural assemblies in the Phanerozoic cover of the Mid-Russian Dislocation Zone.

STRUCTURAL ASSEMBLIES IN THE NORTHEASTERN SEGMENT OF THE MID-RUSSIAN DISLOCATION ZONE

Mega- and macrostructural assemblies. Folds and faults are widespread in the Phanerozoic sedimentary cover of the northeastern segment of the Mid-Russian Zone. They are especially evident within a NE-trending tract 30–50 km wide. The less intense dislocations near the walls of this zone make its contour diffuse and arbitrary.

Upper Permian and Lower Triassic sedimentary rocks largely crop out within this zone (from bottom to top): (1) marine terrigenous and carbonate rocks of the Kazanian Stage (70–130 m); (2) the continental variegated sequence of the Tatarian Stage (>450 m) consisting of three units (the lower unit: sand, silt, and their cemented varieties; the middle unit: intercalating dolomitized limestone, marlstone, and clay; the upper unit: varicolored clay and marlstone with limestone interbeds and lenses of alluvial sand); (3) Lower Triassic continental variegated rocks of the Induan Stage overlying scoured sedimentary rocks of the Tatarian Stage and comprising two units up to 100 m in total thickness (lower unit: alluvial and lacustrine sands with conglomerate interbeds; upper unit: red beds of clay and siltstone). The Jurassic rocks pertaining to the Bathonian and Callovian stages locally occurring in

the southeastern wall of the zone are composed of continental and near-shore marine silty–clayey units, respectively [5, 7]. The rocks in the dislocation zones are enriched in gypsum owing to the high permeability of fractured rocks drained by sulfate solutions. The high sulfate content of the water is caused by dissolution of the Lower Permian evaporites (gypsum, anhydrite, and rock salt of the Artinskian and Kungurian stages), which are not exposed at the ground surface but penetrated by wells.

The central portion of the Mid-Russian Zone is marked by the Rybinsk–Sukhona Megaswell that extends for more than 600 km having a width of 20–40 km (Fig. 2b). The megaswell is complicated by longitudinal and oblique anticlines and swells of the second order, often en-echelon arranged in plan view (Fig. 3). These structural elements are expressed in the configuration of contour lines of Paleozoic reference stratigraphic units and in the attitude of the beds. Against the background of the general northeastern trend of the dislocation zone, the oblique folds are oriented in the ENE and W–E directions. Their echeloned systems often show a left-lateral structural pattern indicative of left-lateral strike-slip faulting along the zone. The amplitude of the anticlines varies from a few tens of meters to 100–200 m at a width of 5–20 km. The aspect ratio of particular swells and anticlines is 3–5. The averaged dip angles at the limbs commonly do not exceed a few degrees, occasionally reaching 10–20°. Many folds are asymmetric. In different segments of the zone, the axial planes of the folds are slightly inclined to the northwest or the southeast. In the lower reaches of the Sukhona River, the megaswell verges to the southeast as a whole (Fig. 4). To the southwest, at the latitude of Vologda, the vergence becomes opposite. Folds of the second order are traced down to the bottom of the Devonian sedimentary rocks, whereas the largest ones are traced to the surface of the crystalline basement [2, 5]. This indicates that halokinesis in the Lower Permian evaporites deformed conformably with over- and underlying rocks is of subordinate importance for folding (Fig. 4b).

Tectonic faults complicate the structure of the megaswell. In particular, these are the extended NE-trending fault zones readily interpreted in aerial photographs and satellite images from tightened-up contour lines of stratigraphic reference units or their disruption (Figs. 2, 3). The largest disturbances of this kind complicate the megaswell limbs and penetrate into the basement merging with the normal fault zones that bound the Riphean grabens. The faults mapped at the ground surface are projected on the corresponding fault zones in the basement, indicating that they remain almost vertical throughout the entire sedimentary cover (2–3 km). In the upper part of the cover, including the Lower Triassic sedimentary rocks and locally developed Middle Jurassic rocks, the vertical separation along the longitudinal faults occasionally reaches 100 m. The aforementioned oblique faults are splays with respect to the longitudinal faults. Their structural position testifies to the left-lateral offset along the longitidinal faults. Taking the vertical separation into account, these disturbances are left-lateral reverse–strike-slip faults (Fig. 3).

Oblique and transverse faults are widespread in the axial part of the Mid-Russian Zone and at its walls. Since they are accompanied by slight offsets of contour lines in plan view without vertical separation, these are strike-slip faults (Fig. 3). The largest fault system of this type is oriented in the W–E direction and traced at the northwestern wall of the Mid-Russian Zone intersecting with the latter in the lower reaches of the Sukhona River (Fig. 2). This system comprises separate strike-slip zones complicated by megalenses and splays. At the intersection with the faults and folds of the Rybinsk–Sukhona Megaswell, the latter reveal right-lateral offset (Fig. 4a). In some places, an opposite situation is noted: the latitudinal strike-slip faults undergo refraction or left-lateral offset at the intersection with the NE-trending faults. In other words, both structural elements reveal indications of almost synchronous development, making up a dynamically conjugate system of right-lateral (W–E-trending) and left-lateral (NE-trending) strike-slip faults. These mapped relationships are confirmed by observations of mesostructural elements (see below).

In the upper beds of the cover and on the erosion surface, the aforementioned faults are most often expressed as wide fracture zones and related steep (~300 m/km) and gentle bends and narrow depressions. The width of some zones attains hundreds of meters or a few kilometers, if the regions of their dynamic effect are taken into account. Experimental data show that the width of the zone of dynamic effect of a deep fault in the rigid basement, which penetrates in overlapping sedimentary cover, may be two times larger than the thickness of the cover [13, 29]. In line with this relationship, the thickness of particular dislocation zones in the Mid-Russian Zone can reach 4–6 km at the surface if the cover thickness is 2–3 km. With rare exceptions, no sharp cutoff of stratigraphic boundaries is observed within such zones. Taking into account that many faults control the morphology of river valleys, it may be suggested that their sutures are often hidden beneath fluvial sediments (Fig. 4). In general, the scattered (dissipative) character of the displacements along the wide fracture zones and regions of their dynamic effect should be stated.

In addition to the attributes mentioned above, the deep character of the faults is supported by a unique finding of Early Mesozoic alkaline ultramafic rocks that cut through the upper beds of the Tatarian Stage in the right wall of the Sukhona River valley in its lower reaches [27]. A lenticular subvolcanic melaleucitite body (sill) up to 3 m thick is confined to the intersection of W–E- and NE-trending faults. A small ring structure is interpreted at this intersection as well (Fig. 4a).

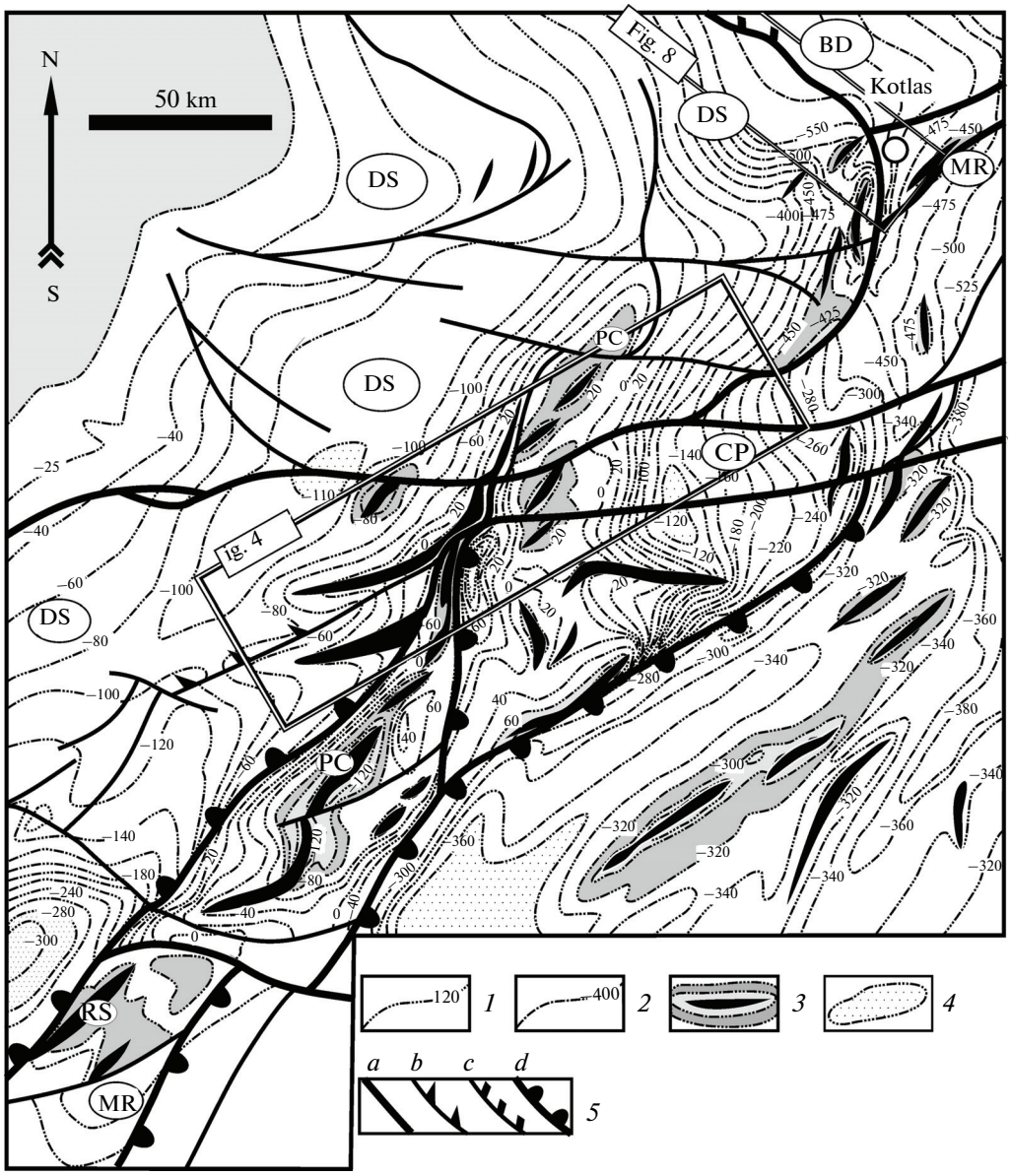

Fig. 3. Structure of the roof of the Kazanian Stage (Upper Permian) and the roof of the Lower Permian in the northeastern part of the scheme, compiled using the data from [4–6]. See Fig. 2b for the area location. (*1, 2*) Contour lines: (*1*) roof of the Kazanian Stage (Upper Permian), (2) roof of the Lower Permian; (*3*) swell or anticline (relative uplift); (*4*) relative trough; (5) fault zones: (*a*) strike-slip, (*b*) reverse, thrust, reverse–strike-slip, (*c*) normal, normal–strike-slip, (*d*) steeply dipping fault or flexure (half-spheres are directed toward subsided wall). See Fig. 2 for abbreviations in figure.

Mesostructural assemblies. Field observations show that postsedimentation mesostructural assemblies related to horizontal tectonic movements are predominant in the dislocation zones considered above. Two types of structural elements are noted: strike-slip zones and zones of nearly horizontal flow and bedding-plane detachment. In many cases, both are conjugated. At the same time, some structural relationships indicate that bedding-plane detachments predated the strike-slip zones. In general, the following structural assemblies are distinguished: (1) synsedimentation structures (D1), (2) early structures of bedding-plane flow (D2), (3) strike-slip structural elements of the main deformation stage (D3), and (4) late, poorly developed strike-slip offsets (D4).

Synsedimentation structures (D1) reveal a number of lithologic attributes indicating tectonic processes during deposition of sedimentary sequences. Primarily, these are sedimentary collapse breccias related to steep tectonic escarpments in the upper part of the Upper Permian section (Tatarian Stage). Lenses of alluvial sand in the Tatarian sediments are often con-

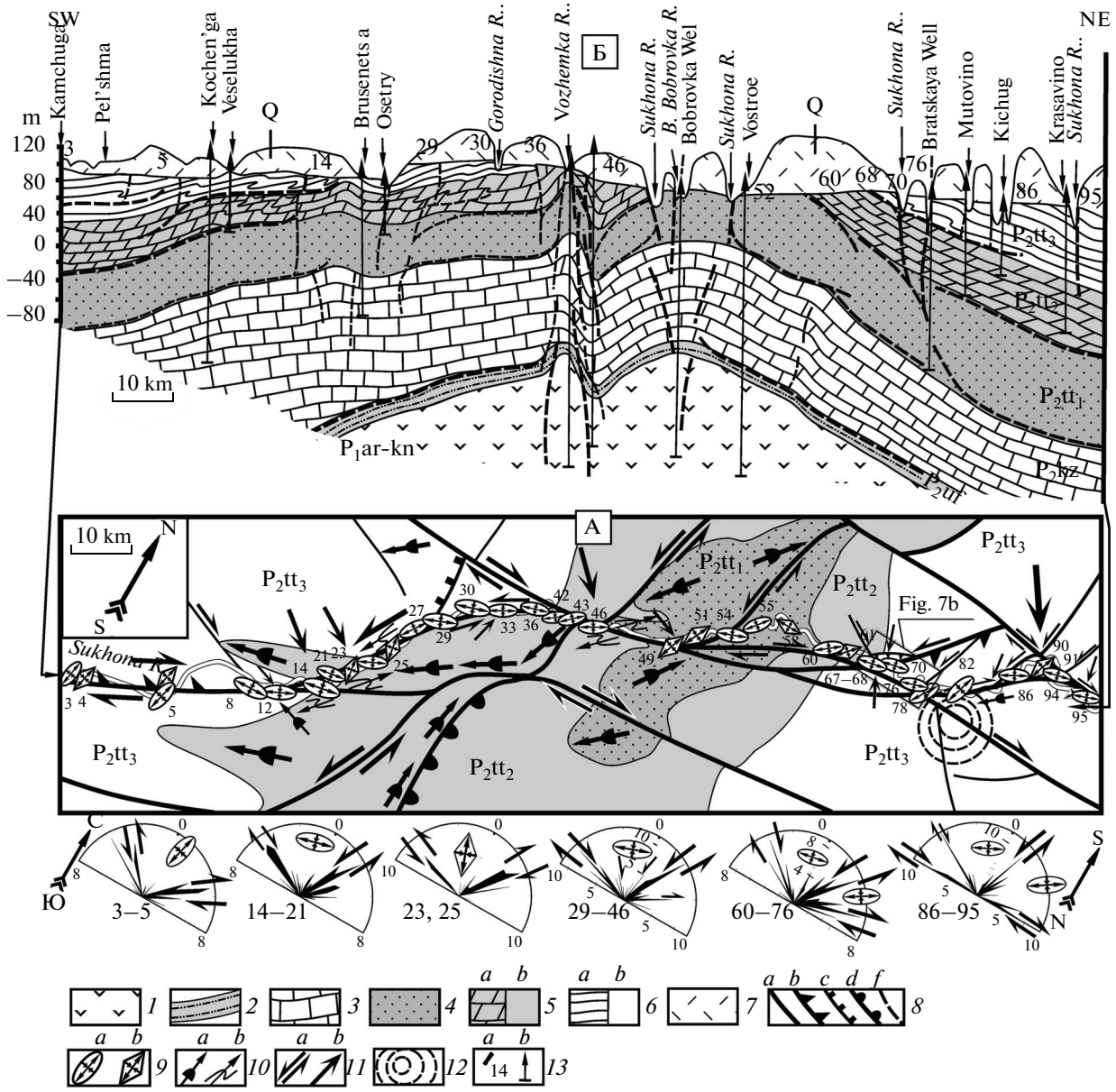

Fig. 4. (a) Geological–structural scheme and (b) section along channel of the Sukhona River along the path of observation route (ops. 3–95) illustrating the structure of the northeastern Rybinsk–Sukhona Megaswell, compiled using the data from [4, 7]. See Fig. 2c for location of area. (*1*) Artinskian and Kungurian stages of the Lower Permian; (*2–6*) Upper Permian stages: (*2*) Ufan, (*3*) Kazanian, (*4–6*) Tatarian, including (*4*) lower, (*5*) middle, and (*6*) upper units: (*a*) in panel (b) and (*b*) in panel (a); (*7*) Quaternary sediments; (*8*) dislocation zones with: (*a*) strike-slip, (*b*) reverse–strike-slip, and (*c*) normal kinematics; (d) steeply dipping fault or flexure (half-spheres are directed toward subsided wall), (e) inferred faults in panel (b); (*9*) observation points and orientation of principal axes of deformation ellipsoid at (*a*) stage D3 and (*b*) D4; (*10*) hinges of (*a*) symmetric and (*b*) asymmetric anticlines and swells; (*11*) direction of (*a*) strike-slip and (*b*) tangential displacement of stage D3; (*12*) inferred area of alkaline ultramafic rocks; (*13*) location of (*a*) observation points and (b) wells in panel (b). Rose diagrams show results of statistical processing of measured orientation of fractures and displacements along them for groups of observation points, whose numbers are indicated near diagrams and in panel (a).

trolled by tightened fracture zones, showing that the channels of ancient streams drained the fault zones. The deformed pebbles of the Tatarian rocks found in the Triassic basal beds also confirm that dislocations developed at the end of the Permian. The kinematics of these presumably Hercynian events remains ambiguous.

Early structures of bedding-plane flow (D2), which do not reveal links with later strike-slip faults D3 are reliably established only sporadically. In the structural patterns and character of tectonites they differ only slightly from the similar structural elements D3 conjugated with the strike-slip zones considered below. Special structures D2 are established reliably only in the

Upper Permian sediments. Their occurrence in the Lower Triassic beds separately from the bedding-plane detachments D3 is doubtful. The age of these structural elements can be determined only as post-Permian.

Strike-slip zones (D3) penetrate the entire section available for observation from the Upper Permian to the Lower Triassic–Upper Jurassic sedimentary rocks and may be regarded as manifestations of the Kimmerian–Alpine tectonic epoch. These are wide belts with locally tightened strike-slip zones of higher orders, fracture systems, and other structural elements, making up regular combinations taken together. The frequency of fractures across the main strike-slip zones is variable and gradually increases with intensity of deformation and approaching relatively narrow (0.1–2.0 m) strike-slip zones of high order, which are expressed in boudinage and foliation of rocks with the formation of breccias, cataclastic rocks, and mylonites. Such zones develop nonuniformly and repeat in groups of 2–3 to 10–15 over a 100-m interval of the section. The fracture zones are localized in the domains of dynamic effect between strike-slip faults. The horizontal offsets along particular shears between strike-slip faults rarely exceed 1–2 cm, whereas they reach a few meters along the high-order strike-slip zones. It cannot be ruled out that strike-slip zones with much greater offsets are hidden beneath the stream channels.

The combinations of fracture systems between the strike-slip zones reflect various stages in the evolution of the latter (Fig. 1c). An outcrop at the mouth of the Upper Yerga River (Fig. 5a) is a characteristic example. Master L-shears cross the entire outcrop or form separate segments connected by echelon-arranged Riedel R-shears and bridge extension structures (pull-apart and normal mini-fault systems). R- and P-shears and tension T-cracks develop as splays along the master L-shears. It is evident that the latter developed as separate segments, each of which began to form with a cascade of short R-shears and then was built up by such shears in the course of progressive growth along the strike. P-shears developed poorly and did not facilitate boudinage that predated the growth of master shears in experiments. The regions of waning shears, where horsetail-type structures consist of small-amplitude (2–5 cm) normal and reverse fractures in the segments of local extension and compression, respectively, are kinematic indications, as well (Fig. 5a). The spatial combinations of conjugate structural elements are shown in a generalized diagram that characterizes the given fracture zone as a fragment of the right-lateral strike-slip fault zone (Fig. 5b). The left-lateral fault zones are not less abundant. They have a similar structure but are distinguished by specularly reflected asymmetry of the auxiliary structures.

Boudinage zones are the most abundant type of strike-slip zones of high order. These structural elements reveal the progressive development of R-, P-, and L-shears, which correspond to the experimental model. A system of trapezium-shaped lenses is formed as a result of their intersection (Fig. 5c). The initial structure composed of R-shears and sporadic embryonal P- and T-fractures is retained at walls of the strike-slip zones. In some cases, the asymmetry of the structure in the boudinage zone itself is not expressed distinctly, whereas in the zone of its dynamic effect it is emphasized by Riedel shears and allows determination of the displacement direction.

In the most intense form, the high-order strike-slip structural elements are manifested in the zones of C–S foliation and sigmoid boudinage (Fig. 5d). In this case, the oblique position and character of S-surface bending with respect to the master strike-slip C-zones are kinematic indicators. In this case, the initial position of the shears is not identified because of their reorientation in the course of rotation in the principal shear plane. Depending on viscosity, S-surfaces appear as poorly developed foliation in clay rocks or thin zones of cataclasis and recrystallization in sandstones and carbonate rocks. They develop nonuniformly, enveloping lenticular bodies of slightly deformed rocks. The sigmoid shape of these lenses testifies to their rotation in line with the direction of slipping (Fig. 5d). Fracture systems of incipient shearing are often observed at the walls of C–S foliation zones.

In many cases, the high-order strike-slip zones developed as a result of several kinematic pulses. This is manifested in the merging of separate fault segments. In addition, initial R- and P-shears and T-fractures are observed to superimpose on late L, S, and C structural elements. In some cases, the local stress field does not change and the previously formed fractures are simply reactivated; in other cases, kinematic inversion with change of slipping sense is noted and the superimposed assemblies D4 may be outlined.

The statistics of observation in the considered territory shows that right-lateral kinematics is inherent to the nearly latitudinal strike-slip zones, whereas the NE-trending zones are characterized by left-lateral offsets (Fig. 4, rose diagrams 3–5, 14–21, 29–46, 60–76, 86–95). The kinematic inversions expressed in superimposed structures commonly do not lead to appreciable rearrangement of strike-slip zones D3, indicating reduced character of deformation D4. Rare exceptions are noted only in local sites (Fig. 4, rose diagrams 23, 25).

Zones of horizontal flow and bedding-plane detachment (D3) are widespread at various levels of the Phanerozoic sequences and are related to strike-slip zones D3. As a rule, they are confined to plastic interbeds (clay, marlstone) intercalating more competent dolomite, limestone, and sandstone. The most intense deformations are noted along the interfaces of rocks different in viscosity. Bedding-plane detachments, thrust faults, and related structural elements develop here. The width of the bedding-plane detachment zones varies from a few centimeters to 10 m and larger.

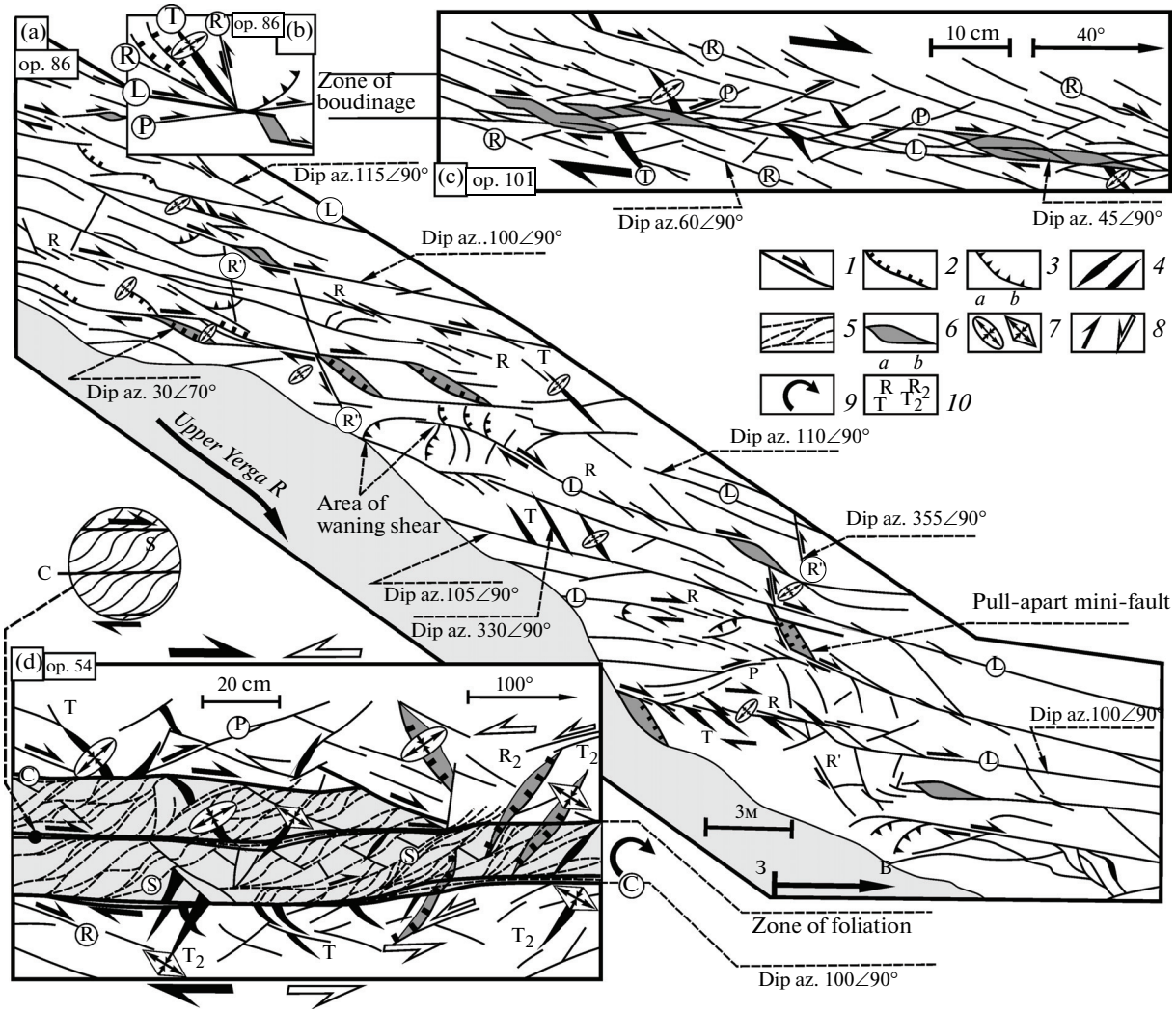

Fig. 5. Horizontal slice of strike-slip zones: (a) fragment of strike-slip fracture zone in Upper Permian marlstone exposed at the mouth of the Upper Yerga River; (b) diagram illustrating spatial relationships of main structural elements in panel (a); (c) fragment of strike-slip zone at the initial stage of boudinage in the Upper Permian dolomite; (d) fragment of C–S foliation zone in the Upper Permian claystone. See Fig. 4a for the location of some observation points.

(*1–4*) fractures with (*1*) strike-slip, (*2*) normal, (*3*) reverse–thrust, and (*4*) pull-apart (tension cracks) kinematics; (*5*) foliation zone; (*6*) mini-depression and sinks related to local extension; (*7*) orientation of principal axes of deformation ellipsoid at (*a*) stage D3 and (*b*) D4; (*8*) direction of strike-slip offsets at stages (*a*) D3 and (*b*) D4; (*9*) direction of rotation; (*10*) notation of kinematic type of fractures at stages (*a*) D3 and (*b*) D4); see Fig. 1 for explanation of these notations.

The observed displacements are within the same limits. Flow zones are traced for many hundreds of meters and gradually wane or pass on a new stratigraphic level. They commonly repeat in the section. In some vertical escarpments about 60 m high, 2–3 levels of bedding-plane detachments and flow of variable intensity are observed.

Tectonites of various types develop in zones of bedding-plane flow depending on the initial viscosity. Clay interbeds are often transformed into shale with characteristic sigmoid and C–S structural elements (Fig. 6a). A gouge with thin striae oriented in the direction of movement is seen on the surface of sliding. Mylonites develop in marlstone and claystone. Interbeds of competent dolomite and limestone undergo volumetric brecciation and boudinage, often making up a tectonic melange together with the adjacent shale (Fig. 6b). Recrystallization, dissolution, and redeposition under stress are inherent to carbonate rocks and the rocks replaced with gypsum. A complex system of fractures along with thin zones of mylonitization and cataclasis is typical of sandstone and siltstone. Sand and plastic rocks often reveal injections penetrating along fractures into the adjacent beds.

Various structural elements are related parageneticaly to zones of bedding-plane detachment and flow. In particular, these are asymmetric and overturned folds and occasionally recumbent and thrust folds

(Fig. 6c). Their postsedimentation nature is emphasized by several attributes: no indications of scouring and variation in the thickness of beds in fold hinges and limbs; geometric ordering and regular spatial arrangement; and spatial and genetic relations to detachments, thrust faults, and cleavage. The possible links of these structural elements to ancient and recent landslides are not within the scope of this paper. The vergence of asymmetric folds characterizes the direction of displacement of the hanging packet of beds and, as a rule, corresponds to horizontal movements in the underlying zones of bedding-plane flow. The latter, sharply interrupting these structural elements from below, appear as sliding surfaces during the formation of drag folds. It is important to emphasize that folds of this type gradually wane upsection, ruling out their formation as a result of glacial loading. In addition, their vergence commonly does not correspond to the southeastern direction of glacier propagation. These structural elements are widespread. Their dimensions and amplitudes vary from 0.5 to 15 m. The degree of compression and asymmetry directly depend on the intensity of bedding-plane flow of rocks.

In the case when a member of beds differing in viscosity is involved in bedding-plane flow, structural disharmony is revealed. Bedding-plane schistosity develops in plastic beds, whereas complex shear systems appear in the adjacent competent beds, including thrust mini-faults and related structures of bed doubling and thrust duplexes, listric and low-angle normal mini-faults cutting the beds into asymmetric boudins (Figs. 6d, 6e). Progressive widening of bedding-plane flow zones along with the formation of conjugate asymmetric folds is noted. As can be seen in the section, the upper structural levels of the flow zone are partly involved in folding, forming a gentle flexure at the base of the asymmetric fold (Fig. 6d). The curvature of the flexure gradually increases upward, and beyond the flow zone it is transformed into an asymmetric fold in the overlying beds. These factors indicate the long-term development of the entire structure in the following succession: (1) formation of the upper level in the zone of bedding-plane flow; (2) gentle bending of beds above this zone; (3) origination of the lower level of bedding-plane sliding that further controls the asymmetric flexure in the overlying beds, including the upper level of the horizontal flow zone, which has become passive.

The case under consideration illustrates an important feature of bedding-plane flow zones expressed in alternation of the segments with predominant structural elements of lateral compression (thrust duplexes) and lateral extension (asymmetric boudins) at the same structural level (Fig. 6d). This feature indicates significantly variable stress fields in the zones of bedding-plane flow.

The spatial relationships between the strike-slip zones (D3) and structural elements of bedding-plane flow (D3) show that they are genetically interrelated. The gradual increase in the intensity of dislocations related to the bedding-plane flow zones with approaching steeply dipping strike-slip zones are noted in many cases. In particular, such relationships were revealed in the lower reaches of the Sukhona River at observation points 65–72 characterizing the structure of the NE-trending strike-slip zone and a wide (up to 3 km) region of its dynamic effect (Fig. 7). A system of asymmetric folds related to the bedding-plane sliding with a gradually increasing degree of tightening toward the main strike-slip fault is revealed in this region. The intensity of bedding-plane flow grows in the same direction, reflected in increasing amplitude of horizontal displacement and width of the corresponding zones, as well as in the character of tectonites.

A system of tight asymmetric, south-verging folds occurs in the northwestern wall of the strike-slip zone (Fig. 7a). Cleavage develops locally parallel to their axial planes. With respect to the master strike-slip zone, the folds are regarded as a system of oblique splays in the common assembly D3 (Fig. 7b). A wide (10 m) zone of bedding-plane flow, along which thrusting in the north-northwestern direction is suggested, was involved in folding. Taking into account the superposition of these structural elements and their opposite vergence, it is supposed that the flow zone and related tectonites were formed during stage D2 before the strike-slip dislocations of stage D3.

A similar situation is noted at the southeastern wall of the zone, but asymmetry and vergence of folds and thrust faults D3 are reflected specularly (Fig. 7b). The above-mentioned bedding-plane flow zone and crowning system of N-verging asymmetric folds develop here as well (Fig. 6d). Thus, the main strike-slip zone is accompanied at the walls by a system of auxiliary folds and thrusts, whose vergence and orientation correspond to the left-lateral offset (Fig. 7b, inset of observation points (ops.) 65–72).

The integral model of strike-slip zones D3 is displayed as a 3D diagram demonstrating the spatial relations of the structural elements in the dynamically coordinated assembly, including the main strike-slip zone, zones of bedding-plane flow, and crowning oblique asymmetric folds at the walls of the strike-slip zone (Fig. 7c).

Such a situation is noted in many cases (ops. 12–14, 36–42, 65–72, 73–76), which allows reliable recognition of structural elements D3 and determination of the kinematics of the strike-slip zones (Figs. 4a, 7b). The ordering in the structural orientation of the folds with respect to the strike-slip zones testifies to their tectonic origin.

In general, the northeastern segment of the Mid-Russian Zone at the upper structural level is a transpressional structural element formed largely during deformation stage D3 related to the Kimmerian–Alpine tectonic epoch. The echeloned oblique folds that complicate the Rybinsk–Sukhona Megaswell

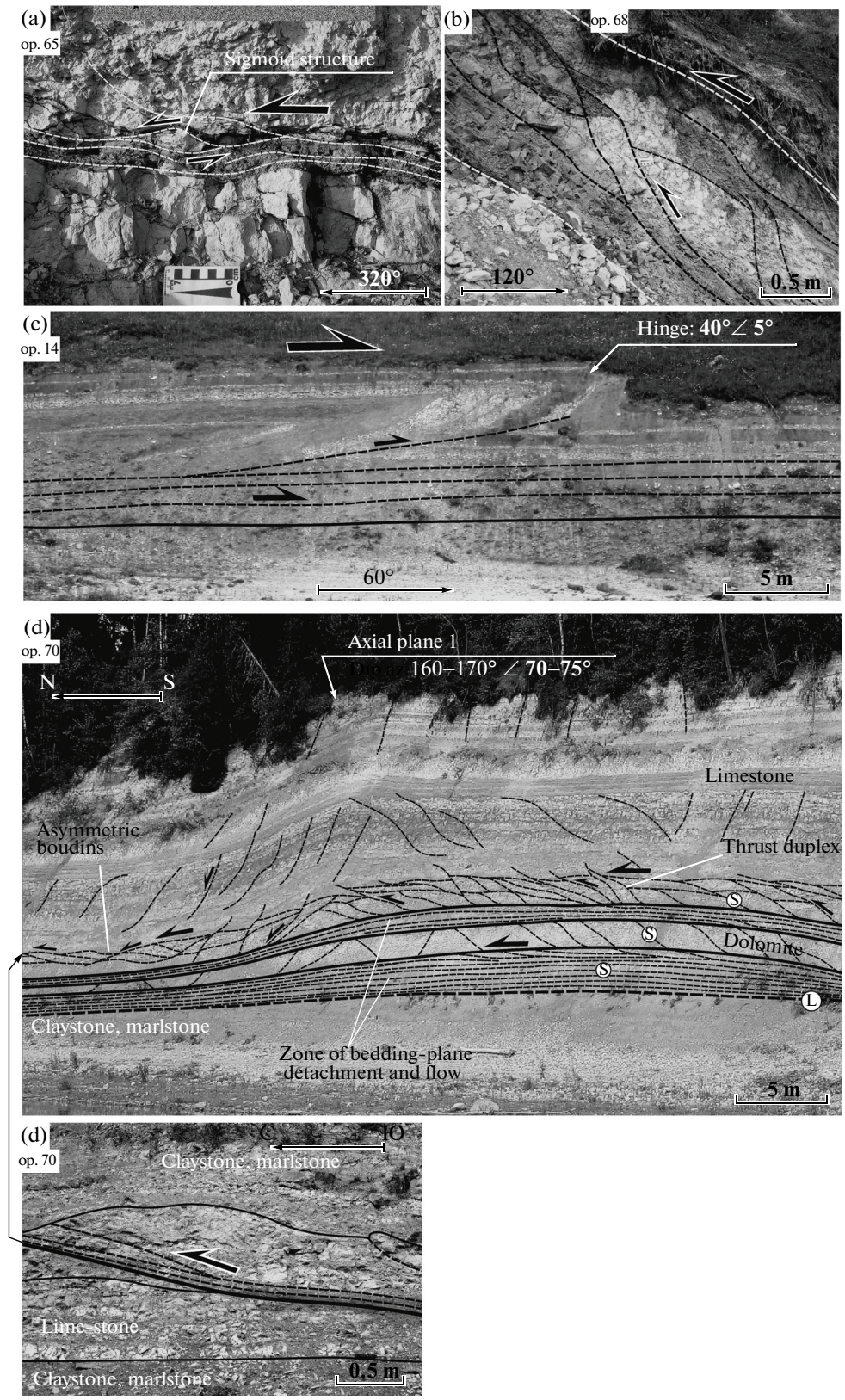

Fig. 6. Photographs of structural elements related to bedding-plane flow and detachment in variegated rocks of the Tatarian Stage (Upper Permian) in the Sukhona River valley (view in section): (a) clay interbed in limestone affected by foliation related to bedding-plane detachment; (b) tectonic melange in the zone of bedding-plane detachment and overthrusting shown in Fig. 7a (op. 68); (c) recumbent asymmetric fold–thrust fault conjugated to detachment and flow zone; (d) structure of bedding-plane detachment, flow zone, and conjugate asymmetric fold; (e) structure of doubling related to bedding-plane flow (close-up of Fig. 6d). See Fig. 1 for symbols and abbreviations.

along its strike and the NE-trending longitudinal left-lateral strike-slip zones were formed during this stage. Near-latitudinal right-lateral strike-slip faults conjugated with longitudinal left-lateral faults are inscribed into the structure of the Mid-Russian Zone, as well.

CONJUGATION OF THE MID-RUSSIAN AND BELOMORIAN–DVINA ZONES

The northeastern segment of the Mid-Russian Zone is conjugated with the Belomorian–Dvina Zone, similar in many respects (Fig. 2). The latter also inherit the spatial position of the Paleoproterozoic mobile belt and the Riphean rift system, being superimposed thereon. The Phanerozoic sedimentary cover, however, does not reveal an inversion uplift resembling the Rybinsk–Sukhona Megaswell. Conversely, the present-day Belomorian–Dvina Zone is a neotectonic depression bounded by a system of normal–strike-slip faults and filled with Quaternary sediments [9]. In general, both tectonic zones frame the Dvina–Sukhona Block, a giant wedge in plan view.

The Belomorian–Dvina Zone is traced southeastward from the Kandalaksha Bay of the White Sea to the junction with the Mid-Russian Zone at the headwater of the Severnaya Dvina River near the city of Kotlas. The junction region is a depression corresponding to the wide valley of the Severnaya Dvina River and bounded by normal–strike-slip faults (Figs. 2b, 2c). At the southwestern wall of the depression, these faults cut off Upper Permian and Lower Triassic rocks and occasionally penetrate into Quaternary sediments with the formation of steep scarps and active landslides along them (Fig. 8a). Judging from the morphology of the valley, the channel of the Severnaya Dvina River gradually migrated approaching these scarps. This testifies to the more active subsidence of the southwestern wall of the depression along the fault zones. Low-amplitude normal and reverse fractures with a strike-slip component are widespread at the walls of these zones, being oriented obliquely and normally to the main normal–strike-slip faults (Fig. 8a).

A system of folds expressed in low-angle (up to 6°) tilting of beds and alternation of Permian and Triassic rocks at the same hypsometric level (Fig. 8b) is noted here. This phenomenon was considered previously as a result of erosion of Permian sedimentary rocks in the course of the deposition of the Lower Triassic fluvial sand in the scours, which are interpreted now as synclines. The morphology of cross-bedding in the basal Triassic beds makes it possible to determine the direction of ancient streams. It turns out that in some extended intervals they flowed across sinks and uplifts (Fig. 8b, ops. 372–376). These observations confirm the tectonic origin of these structural elements and allow them to be viewed as gentle oblique fault-line folds that postdated the accumulation of Lower Triassic sediments.

The mesostructures in the Permian and Triassic rocks reveal generally similar orientation of the fracture systems (Fig. 8b, rose diagram I–II). The NW-trending fracture zones have the left-lateral component of displacement dominating over the normal component. The intensity of these dislocations in the Lower Triassic sand decreases markedly, but in coeval claystone it is comparable to the intensity of dislocations in the Permian sedimentary rocks. The direct penetration of strike-slip zones from Permian rocks into Triassic basal beds is noted. Thus, there is no sharp structural unconformity between Permian and Triassic rocks. The variable intensity of dislocations is caused by the rheological properties of Triassic loose sand. As was mentioned above, the Hercynian diastrophism took place at the end of the Tatarian Age, but its manifestation is yet not documented in the structural and kinematic assemblies.

In general, the southeastern segment of the Belomorian–Dvina Zone is a left-lateral transtensional structural element. Judging from the relationships with the Permian and Triassic sedimentary rocks, the dislocations of this zone most likely belong to stage D3 and probably D4 of the Kimmerian–Alpine tectonic epoch. The structural position of oblique folds and reverse–strike-slip faults accompanying the main zone is consistent with the left-lateral offset (Fig. 8a). The orientation of the normal–strike faults at the walls of this zone is more complex and some of them probably formed earlier.

Close to Kotlas, the normal–strike-slip faults in the southwestern wall of the Belomorian–Dvina Zone smoothly change their northwestern trend and become nearly N–S-trending (Fig. 8a). Thus, the depression wanes and the Severnaya Dvina River basin narrows. The master faults, curvilinear in plan view, retain the left-lateral component of displacement (Fig. 8b, rose diagram III). Such a situation is traced up to the merging of these strike-slip faults with the NE-trending dislocations of the Mid-Russian Zone.

As a result of the junction of the Mid-Russian and the Belomorian–Dvina zones, a common structural element arcuate in plan view and facing the east-southeast by its prominence is formed. At the maximal curvature of this arc, the meridional swell-shaped structural elements appear, testifying to the latitudinal tectonic compression, probably under effect of the Dvina–Sukhona Block (Fig. 3).

DISCUSSION AND DYNAMIC RECONSTRUCTIONS

The data considered above show that the Mid-Russian Zone is a deep, long-lived structural unit formed against the background of variable tectonic settings: (1) Late Paleoproterozoic collisional events; (2) Late Riphean–Early Vendian epicontinental rifting; (3) Late Vendian–Early Triassic platform tectogenesis, when local horst-like uplifts and depressions were formed

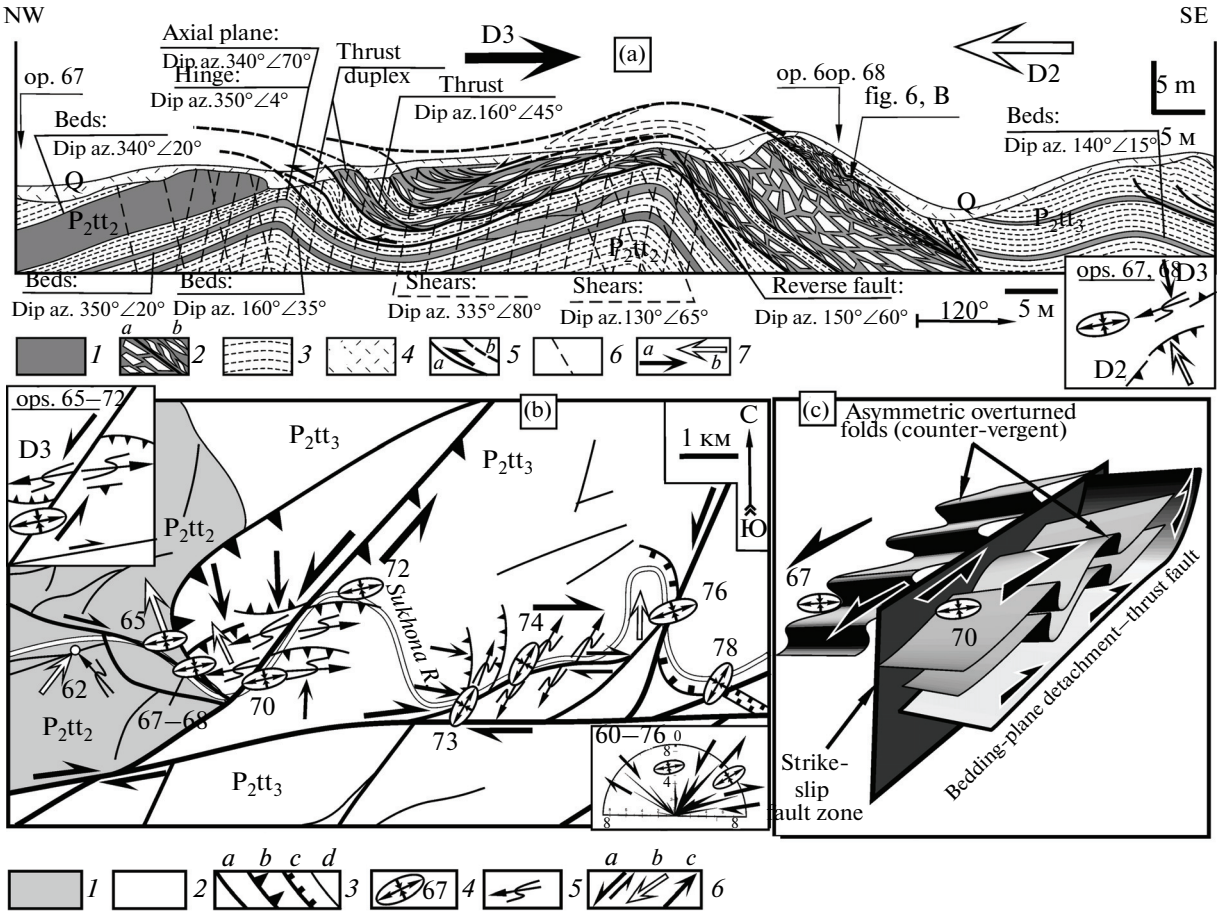

Fig. 7. (a) Geological and structural section, (b) structural scheme, and (c) 3D diagram illustrating relationships of strike-slip fault zones and structures of bedding-plane flow in the lower reaches of the Sukhona River in intervals of observation points 62–78. See Fig. 4a for location of panel (b).

Panel (a): (*1–3*) rocks of the Tatarian Stage of Upper Permian: (*1*) limestone, (*2*) brecciated (*a*) and foliated (*b*) limestones, (*3*) claystone and marlstone; (*4*) Quaternary sediments; (*5*) faults and direction of displacement along them: (*a*) proved and (*b*) inferred; (*6*) cleavage; (*7*) direction of tangential displacement (thrusting): (*a*) late (D3) and (*b*) early (D2) stages. Panel (b): (*1, 2*) rocks of the Tatarian Stage of the Upper Permian: (*1*) upper and (*2*) middle units; (*3*) dislocation zones with predominant (*a*) strike-slip, (*b*) reverse–thrust, and (c) normal kinematics; (d) lineaments with unclear kinematics; (*4*) observation points and orientation of principal deformation axes in Permian sedimentary rocks; (*5*) hinge of asymmetric anticline; (*6*) directions of (*a*) strike-slip, (*b, c*) tangential displacements during stages (*b*) D2 and (*c*) D3. The insets of ops. 65–72 and ops. 67, 68 show the spatial relationships of the main structural elements in the corresponding observation points.

against the background of general subsidence of the Moscow Syneclise; and (4) Mesozoic–Cenozoic within-plate reactivation [2, 5, 21–23, 28].

The structural and kinematic data make it possible to characterize the late stage in the evolution of the Mid-Russian Zone in more detail. At present, it is hardly feasible to determine the age interval of deformation more precisely than Mesozoic–Cenozoic. Structural elements D3 and D4 corresponding to this epoch are reliably traced in the Upper Permian and Lower Triassic sedimentary rocks. As follows from drilling results and geological mapping, the deformations penetrated into the Middle–Upper Jurassic beds. No younger strata except Quaternary occur in the studied zone. Glacial dislocations and postglacial disturbances in Quaternary sediments are sporadic and insufficient for tectonic interpretation. The recently found occurrence of alkaline ultramafic rocks presumably related to Early Mesozoic reactivation [27] expands the possible chronological interval of deformation.

The signs of intense deformation D3 are clearly expressed in the present-day topography as lineaments, positive and negative morphostructures. The transpressional Mid-Russian Zone is manifested as a rise or a ridge, whereas the transtensional Belomorian–Dvina Zone, as a recent depression. Taking into account that the relief of this territory was formed in the Alpine time [5], deformations D3 and D4 may be

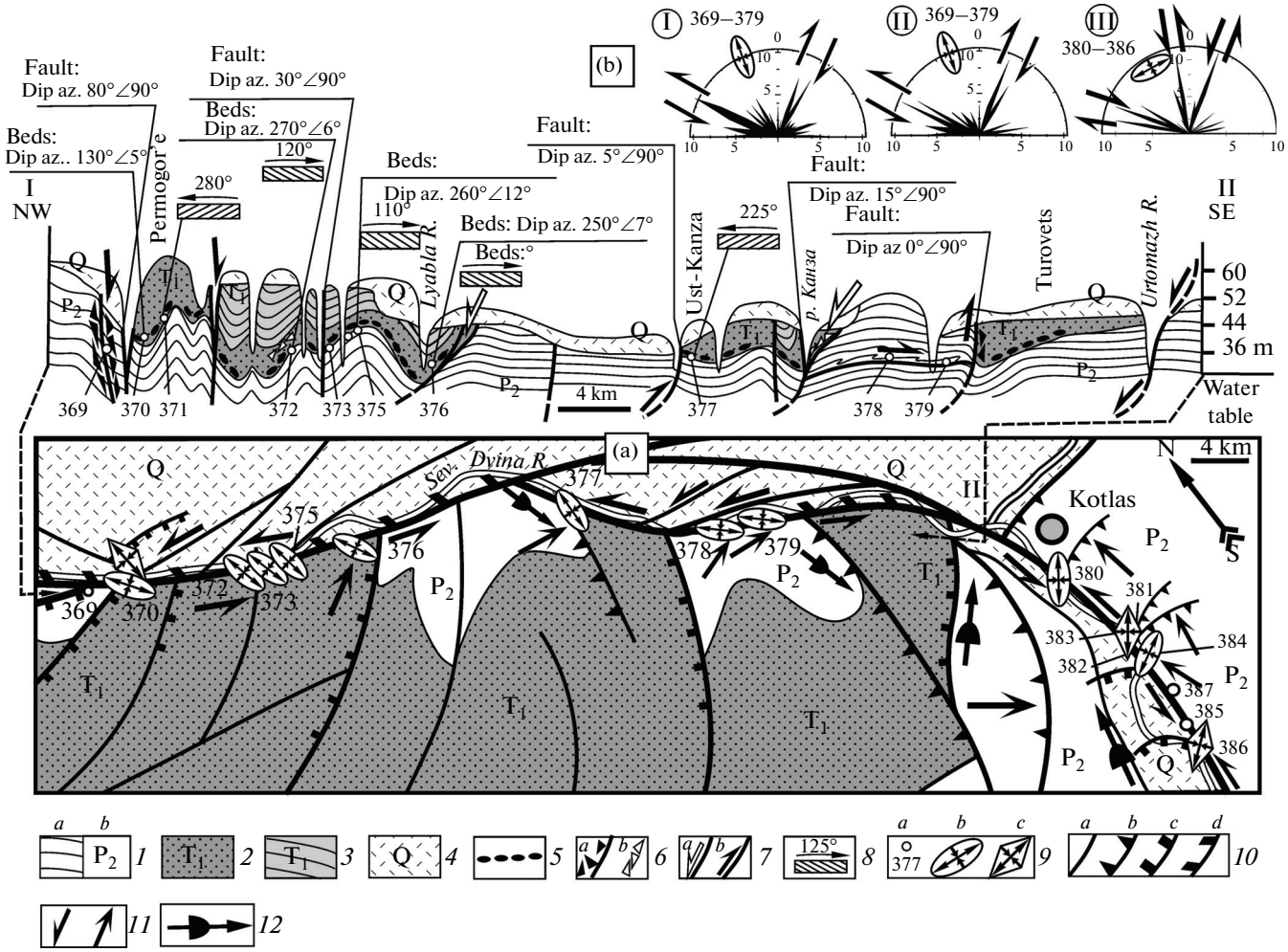

Fig. 8. (a) Geological–structural scheme and (b) section along line I–II illustrating the structure of the southeastern segment of the Belomorian–Dvina Zone, compiled using the data from [6, 7]. See Fig. 2c for area location. (*1*) rocks of the Tatarian Stage of the Upper Permian: (*a*) in panel (b) and (*b*) in panel (a); (*2, 3*) Lower Triassic rocks; (*2*) sand and (*3*) claystone; (*4*) Quaternary sediments; (*5*) conglomerate unit; (*6a*) tectonic and (*6b*) sedimentary breccias; (*7*) faults and directions of displacement along them at the (*a*) early and (*b*) late stages; (*8*) inclination of cross-bedding in sandstone and reconstructed direction of paleostream flow; (*9a*) observation points and (*b, c*) orientation of principal axes in deformation ellipsoid in the (*b*) Permian and Triassic sedimentary rocks and (*c*) Quaternary sediments; (*10*) dislocation zones with predominant (*a*) strike-slip, (*b*) reverse, (*c*) normal, and (*d*) normal–strike-slip kinematics; (*11*) direction of (*a*) strike-slip and (*b*) tangential displacements; (*12*) swell and anticline axes. Rose diagrams show the results of statistical processing of the measured orientation of fractures and displacements along them for groups of observation points, whose numbers are shown near the diagrams and in panel (a) (diagram I, III in the Upper Permian rocks and diagram II in the Lower Triassic rocks).

regarded with a high probability as a manifestation of Alpine within-plate reactivation.

Structural and kinematic studies have shown that the structural assemblies D3, which predetermine the main present-day structural features of the sedimentary cover, are related largely to horizontal displacements developing in the context of two dynamic systems: (1) widely scattered zones of dissipative shearing and (2) zones of bedding-plane flow and detachment combined with related folds and faults that frequently occur at almost all levels of the Phanerozoic cover accessible for observation. These systems reflect two forms of structural manifestation of dissipative-type shearing, which develop either in the vertical plane (strike-slip faulting) or in the horizontal plane (low-angle detachment). Their distinct spatial position is caused by the structural and rheological properties of rocks. The wrench fault zones inherit the tectonic divisibility of the basement, whereas the zones of horizontal flow inherit the contrasting rheological properties of the bedded rocks in the sedimentary cover.

The strike-slip fault zones and the zones of bedding-plane flow are dynamically conjugated systems, which provide general lateral transfer of rock masses along the vertical and horizontal surfaces, respectively (Fig. 7c). The total dissipative shear deformation in

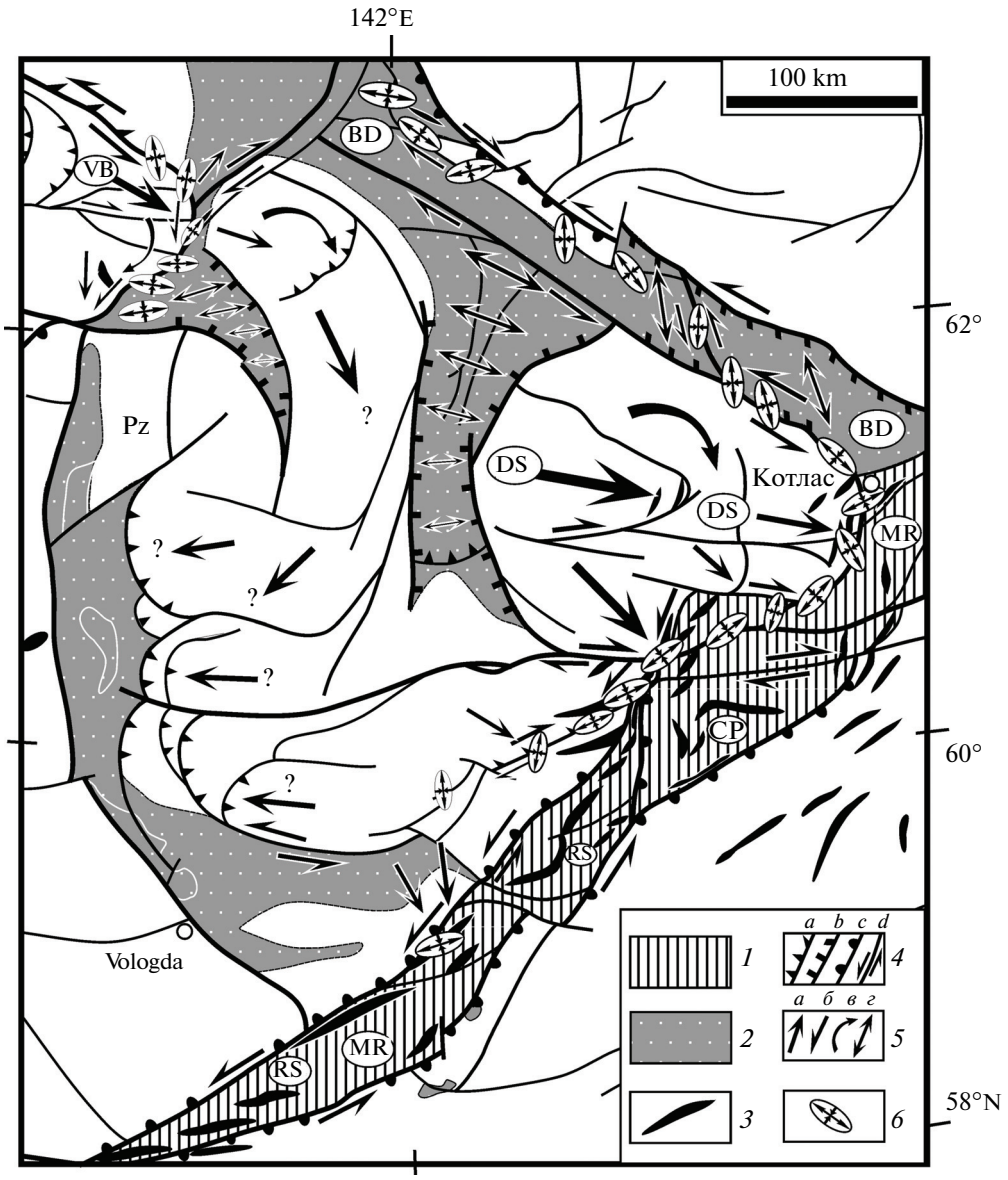

Fig. 9. Structural–kinematic scheme for the Kimmerian–Alpine epoch in evolution of the Mid-Russian dislocation zones and conjugate structural elements. (*1, 2*) Dislocation zones: (*1*) transpressional, (*2*) transtensional; (@3) anticline or swell; (4) fault zones: (*a*) reverse and thrust, (*b*) normal, (*c*) steeply dipping fault or flexure (half-spheres are directed toward subsided wall), (d) strike-slip; (*5*) direction of displacements: (*a*) tangential, (*b*) strike-slip, (c) rotational, (d) pull-apart; inferred displacements are indicated by question mark; (*6*) orientation of principal axes of deformation ellipsoid for stage D3. See Fig. 2 for abbreviations.

these systems encompasses huge rock massifs and is a result of 3D tectonic flow of rocks in the sedimentary cover.

Consider the localization of the structural assemblies of the Kimmerian–Alpine epoch on the basis of structural and kinematic data. The main tectonic elements of the territory are the Mid-Russian and the Belomorian–Dvina dislocation zones. Merging near Kotlas, they frame the Dvina–Sukhona Block, a giant wedge in plan view (Fig. 9). Both zones are dominated by strike-slip dislocations developing in different regimes. The Mid-Russian Zone is a transpressional (shear + compression) structural element characterized by combination of en-echelon arranged oblique folds of the Rybinsk–Sukhona Megaswell and longitudinal reverse–strike-slip faults largely with left-lateral offsets. The latitudinal right-lateral faults conjugated with left-lateral faults are inscribed into this structural unit. The Belomorian–Dvina Zone is a transtensional (shear + extension) left-lateral structural element expressed in a linear depression bounded by normal–strike-slip faults. Broadly speaking, the mutual arrangement of both zones indicates general compression in the NW–SE direction. At the same

time, the local stress distribution is much more complex, testifying to the dynamically differentiated tectonic settings (Fig. 9).

The junction of the Mid-Russian and the Belomorian–Dvina zones is an arcuate (in plan view) structural element facing east-southeast by its prominence (Fig. 9). The swell-like structural elements in the most curved segment indicate tectonic pumping and indenting of the Dvina–Sukhona Block into this region. These displacements are consistent with strike-slip offsets at the walls of the indentor: left-lateral in the Belomorian–Dvina Zone and right-lateral along the latitudinal strike-slip faults complicating the northeastern portion of the Mid-Russian Zone (Fig. 9). The left-lateral displacements along the latter are probably related to a general clockwise rotation of the Dvina–Sukhona Block in the process of its indenting to the east-southeast. This is indicated by the wedge-shaped (in plan view) depressions in the western part of the block. The opening of these depressions corresponds to the rotation of the block (Fig. 9).

In all of the aforementioned structural attributes, the Dvina–Sukhona Block may be considered a special category of structural element of within-plate horizontal displacement termed *plate–flow* by Leonov [15]. The appearance of such a block in the considered territory is not accidental. A substantially similar block of the Vetreny (Wind) Belt 400 km to the northwest is a jut of the crystalline basement of the Baltic Shield (Figs. 2b, 9). This structural element, considered in [11], and the Dvina–Sukhona Block probably make up a system of horizontal mass transfer to the southeast or a common, complexly built plate-flow.

The dynamic interpretation discussed above is consistent with a model of the southeastern displacement of the EEP as a response to propagation of the Atlantic Rift to the Arctic and gradual opening of the Arctic spreading zone [12, 17]. As is suggested in [12], these displacements took place during the Alpine epoch of plate evolution due to the right- and left-lateral offsets along its western boundary (Tornquist Line) and eastern boundary (the Urals, Timan Belt ?). The structural data show that the plate did not move to the southeast as a whole. The motion was differentiated and volumetric, as follows from the structural assemblies in the sedimentary cover; the existence of the Mid-Russian and Belomorian–Dvina dislocation zones that dissect the plate; and the manifestation of structural elements of horizontal displacement, e.g., the Dvina–Sukhona plate-flow. The mechanism of stress transfer from the active plate boundaries by thousands of kilometers to the inner regions remains a weak point in this analysis. The solution of this problem requires more extensive information on the tectonics of the northeastern EEP, which is beyond the scope of this paper.

CONCLUSIONS

(1) The Mid-Russian Zone is a deep, long-lived structural element formed against the background of variable tectonic settings: (1) Late Paleoproterozoic collisional events; (2) Late Riphean–Early Vendian epicontinental rifting; (3) Late Vendian–Early Triassic platform tectogenesis, when local horst-like uplifts and depressions were formed against the background of general subsidence of the Moscow Syneclise; and (4) Mesozoic–Cenozoic within-plate reactivation.

(2) During the final Kimmerian–Alpine epoch of its evolution, the Mid-Russian Zone developed as a left-lateral transpressional structural element, where 3D dissipative shear deformation provided horizontal transfer of rocks in Phanerozoic sedimentary cover. Dislocations were manifested in the form of scattered strike-slip faulting and bedding-plane tectonic flow.

(3) The Mid-Russian and the conjugate Belomorian–Dvina zones make up an arcuate (in plan view) system of within-plate horizontal displacement—the Dvina–Sukhona plate-flow with transfer of rock masses to the southeast.

ACKNOWLEDGMENTS

This study was supported by the Russian Foundation for Basic Research (project nos. 06-05-64848, 07-05-01158), the Division of Earth Sciences, Russian Academy of Sciences (program no. 10), and the Foundation for the Support of Russian Science.

REFERENCES

1. V. S. Burtman, A. V. Luk'yanov, A. V. Peive, and S. V. Ruzhentsev, "Horizontal Displacement along Faults and Some Methods of Their Study," in *Faults and Horizontal Movements of the Eart's Crust* (Acad. Sci. USSR, Moscow, 1963), pp. 5–34 [in Russian].
2. R. G. Garetsky and M. A. Nagorny, "Main Stages in Evolution of the Moscow Syneclise," Litosfera, No. 2, 14–24 (2006).
3. *Hypsometric Map of the Crystalline Basement Surface in the Central and Northern East European Platform on a Scale 1 : 2500000*, Ed. by V. P. Orlov and D. L. Fedorov (VSEGEI, St. Petersburg, 2001) [in Russian].
4. *State Geological and Hydrogeological Map of the USSR on a Scale 1 : 200000, Mezen Series, Map Sheets R-38-XXXI, R-38-XXXII, R-38-XXXIII; O-38-I; O-38-II. Explanatory Notes* (VSEGEI, Leningrad, 1989) [in Russian].
5. *State Geological Map of the Russian Federation on a Scale 1 : 1000000 (New Series), Map Sheet O-37, (38) (Nizhnii Novgorod). Explanatory Notes* (VSEGEI, St. Petersburg, 2000) [in Russian].
6. *State Geological and Hydrogeological Map of the USSR on a Scale 1 : 200000, Mezen Series, Map Sheet P-38-XXIX* (VSEGEI, Leningrad, 1988), [in Russian].
7. *State Geological Map of the USSR on a Scale 1 : 1000000 (New Series), Map Sheet P-38 (Velikii Ustyug). Explanatory Notes* (Nedra, Moscow, 1965) [in Russian].

8. *Gravimetric Map of Russia on a Scale 1: 5000000,* Ed. by O. V. Petrov (VSEGEI, St. Petersburg, 2004) [in Russian].
9. D. S. Zykov, S. Yu. Kolodyazhny, and A. S. Baluev, "Indications of Horizontal Neotectonic Mobility of the Basement in the Belomorian Region," Byull. Mosk. O–va Ispyt. Prir., Otd. Geol. **83** (2), 15–25 (2008).
10. S. Yu. Kolodyazhny, *Structural and Kinematic Evolution of the Southeastern Baltic Shield* (GEOS, Moscow, 2006) [in Russian].
11. S. Yu. Kolodyazhny, D. S. Zykov, and M. G. Leonov, "Structural–Kinematic Parageneses of the Basement and Cover at the Southeastern Margin of the Baltic Shield," Geotektonika, **41** (6), 3–22 (2007) [Geotectonics **41** (6), 423-439 (2007)].
12. M. L. Kopp, *Mobilistic Neotectonics of Platforms in Southeastern Europe* (Nauka, Moscow, 2005) [in Russian].
13. R. B. Krapivner, *Rootless Neotectonic Structural elements* (Nedra, Moscow, 1986) [in Russian].
14. P. N. Kropotkin and V. N. Efremov, "Tectonic Stresses at Platforms and Global Variations of Seismicity," Geotektonika **27** (5), 34–36 (1993).
15. M. G. Leonov, *Tectonics of the Consolidated Crust* (Nauka, Moscow, 2008) [in Russian].
16. Yu. G. Leonov, "Tectonic Criteria of Interpretation of Seismic Reflectors in the Lower Continental Crust," Geotektonika **27** (5), 4–15 (1993).
17. Yu. G. Leonov, "Stresses in the Lithosphere and Intraplate Tectonics," Geotektonika **29** (6), 3–21 (1995).
18. Yu. G. Leonov, O. I. Gushchenko, M. L. Kopp, and L. M. Rastsvetaev, "Relationship between the Late Cenozoic Stresses and Deformations in the Caucasus Sector of the Alpine Belt and Its Northern Foreland," Geotektonika **35** (1), 36–59 (2001) [Geotectonics **35** (1), 30–50 (2001].
19. A. V. Luk'yanov, *Structural Occurrences of Horizontal Movements in the Earth's Crust* (Nauka, Moscow, 1965) [in Russian].
20. A. V. Luk'yanov, *Ductile Deformation and Tectonic Flow in the Lithosphere* (Nauka, Moscow, 1991) [in Russian].
21. M. V. Mints, I. B. Filippova, A. K. Suleimanov, et al., "The East European Craton – Paleoproterozoic Accretionary–Collisional Orogen," in *Proceedings of XXXIII Tectonic Conference on Tectonics of the Earth's Crust and Mantle and Tectonic Localization of Mineral Resources* (GEOS, Moscow, 2005), pp. 452–456 [in Russian].
22. M. V. Mints, I. B. Filippova, A. K. Suleimanov, et al., "Deep Structure of the Early Precambrian Crust of the East European Craton: Formation of Over- and Underthrust Structural Elements in the Inner Part of the Supercontinent Related to Accretion and Collision " in *Proceedings of XXXVIII Tectonic Conference on Tectonics of the Earth's Crust and Mantle and Tectonic Localization of Mineral Resources* (GEOS, Moscow, 2005), Vol. 1, pp. 452–456 [in Russian].
23. M. A. Nagorny, *Tektonics of the Volyn–Mid-Russian System of Troughs* (Nauka i Tekhnika, Minsk, 1990) [in Russian].
24. L. M. Rastsvetaev, "Paragenetic Method of Structural Analysis," in *Problems of Structural Geology and Physics of Tectonic Processes. Chast' 2* (Geol. Inst., Moscow, 1987), Part 2, pp. 173–235 [in Russian].
25. L. A. Sim, "Recent Stress Fields of the East European Platform," Litosfera, No. 5, 100–107 (1996).
26. *Structural Map of the Roof of the Vereya Unit of the Moscow Stage, Middle Carboniferous*, Ed. by V. V. Bronguleev (Nedra, Moscow, 1986) [in Russian].
27. A. I. Trufanov, "The First Finding of the Early Mesozoic Alkaline Ultramafic Igneous Rocks in the North of the Russian Plate," Region. Geol. Metal., No. 30/31, 57–61 (2007).
28. N. P. Chamov, "Tectonic History and a New Evolution Model of the Mid-Russian Aulacogen," Geotektonika **39** (3), 3–22 (2005) [Geotectonics **39** (3), 169–185 (2005)].
29. S. I. Sherman, S. A. Bornyakov, and V. Yu. Buddo, *Regions of Dynamic Effects of Faults (Modeling Results)* (Nauka, Novosibirsk, 1983) [in Russian].
30. M. Doblas, "Slickenside Kinematic Indicators," Tectonophysics **295**, 187–197 (1985).
31. M. A. Naylor, G. Mandl, and C. H. K. Sijpesteijn, "Fault Geometries in Basement-Induced Wrench Faulting Under Different Initial Stress States," J. Struct. Geol **7**, 737–752 (1986).

SPELL: 1. Burtman